PROCEEDINGS OF SCIENCE

m_c (and m_b) from lattice QCD

Andrew T. Lytle*

Department of Physics, University of Illinois at Urbana-Champaign, Urbana, Illinois, 61801, USA

E-mail: atlytle@illinois.edu

Quark mass determinations based on lattice QCD simulations have continued to make strides in recent years. Here I review that progress with a focus on developments computing the charm (and bottom) quark masses since the 2015 edition of CHARM. These advances have resulted in groups now quoting (sub-)percent-level precision for these quantities, and, importantly, using a variety of techniques subject to differing systematic uncertainties. Improvements to quantify the effects of QED are also now being included. I will highlight three of the strategies being used to determine m_c at this level of precision.

**** 10th International Workshop on Charm Physics (CHARM2020), ****
**** 31 May - 4 June, 2021 ****
**** Mexico City, Mexico - Online ****

*Speaker

PoS(CHARM2020)013

1. Introduction

When preparing this talk, I returned to materials I had prepared from the 2015 edition of the CHARM conference. It was natural to frame the presentation in terms of the progress that has been made since that iteration, and I was pleasantly surprised just how much progress there has been on the topic. This progress has been partially incremental, in that precision for various calculations continues to improve as time goes on due to increases in computing power, refinement of techniques, more ensembles with finer lattice spacings, etc. – but importantly the number of techniques being used to achieve quark masses at a high level of precision has increased, and these results are on the whole in agreement with one another despite the very different approaches (and corresponding systematic sources of uncertainty). This gives confidence in the robustness of these results and in the reliability of the error estimates, and taken together represents a significant achievement of the lattice community as a whole.

The goal of this talk then is to summarize the recent results in the field, paying attention to the various methodologies being used. In this talk I will focus primarily on three different methods. (I will also rely on FLAG averages, and specifically highlight new results available since the last FLAG review [2].) These are the methods of current-current correlators (which was the focus of the Charm 2015 review [3]), RI/(S)MOM intermediate schemes, and MRS masses. Sec. 2 will briefly review the definition of quark mass parameters and how they are determined from lattice QCD simulations. Sec. 3 comprises the bulk of the article focused on charm mass, and goes into some detail on the methods used by different groups. Sec. 4 provides a brief update on the state-of-the-art in mass determinations of the bottom quark. Sec. 5 summarizes the results and discusses the future of these calculations.

2. Quark mass and LQCD

Quark masses are fundamental parameters that arise in the Standard Model from interaction with the Higgs field, and the precision determinations of heavy quark masses are needed to stringently test Standard Model predictions for Higgs-fermion couplings [1]. Because of confinement in QCD, quark masses cannot be measured directly but must be related to physical observables, such as hadron masses, via theoretical tools. Quark mass parameters are scheme and scale dependent quantities, and are typically quoted in the $\overline{\text{MS}}$ scheme. In this document I will try to make explicit this dependence, for the charm and bottom results are typically quoted at the scale of the quark itself, i.e. $m_c^{\overline{\text{MS}}}(m_c)$, $m_b^{\overline{\text{MS}}}(m_b)$, though sometimes other choices are made such as $m_c^{\overline{\text{MS}}}(3\text{ GeV})$. The quark mass definitions also depend on the number of quarks in the sea n_f, and I've also tried to make note of this where applicable.

In lattice QCD simulations, quark masses are dimensionless input parameters specified in terms of the lattice spacing a, i.e. $am_{ud,0}$, $am_{s,0}$, $am_{c,0}$. The subscript '0' on these quantities is to indicate they are bare input quantities, and depend on the details of the regularization being employed. In particular they have no well-defined physical meaning, but must be related to renormalized quark masses defined in the continuum. (In contrast quark mass *ratios* are physically meaningful, and can be used for example to obtain m_b from m_c and a determination of m_b/m_c.) In simulation each input quark mass is tuned to reproduce a physical quantity, for example $am_{ud,0}$ may be tuned to

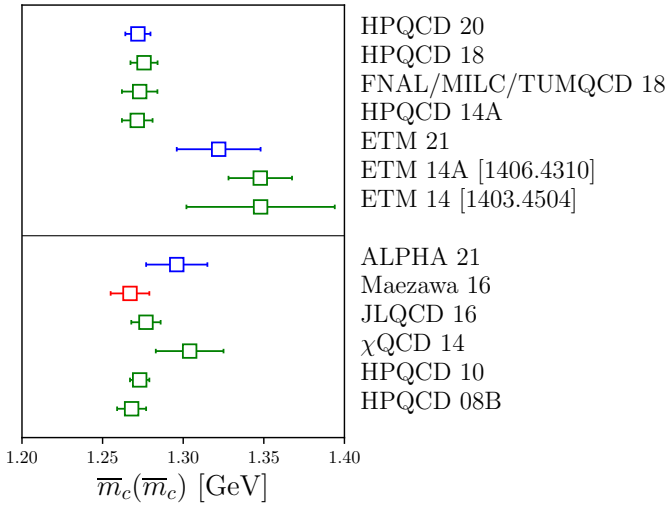

Figure 1: Summary plot of charm mass determinations from the lattice, adapted from 2019 FLAG review. The top (bottom) panel gives results based on gauge configurations with $n_f = 4$ ($n_f = 3$) quark flavors in the sea. New entries published after the review are labelled in blue while the other entries maintain the green/red color designation given by FLAG.

reproduce the pion mass, while $am_{c,0}$ may be tuned to reproduce the J/ψ mass. After these tunings, and a measurement of the lattice spacing, the remaining observables are predictions of the theory of QCD. The ability to dial the quark input parameters and measure the resulting change in physical quantities is one of the reasons lattice simulations are well-suited to precision mass determinations. In particular we will see that being able to map out physical dependences on fictitious heavy quark masses $am_c < am_h < am_b$ is useful. How to make the connection between bare quantities in simulation, and the continuum renormalized quantities, will be explored in the subsequent sections.

3. Charm quark mass

Since 2015 the number of lattice charm mass determinations has more than doubled from 6 to 13, including three since the 2019 FLAG review. The situation is summarized in Fig. 1, where I have updated the results of the FLAG review to reflect these new entries. For the purposes of the talk I would like to especially focus on the four results at the top of the figure, which all separately claim percent-level uncertainty, and remarkably are arrived at through three completely different techniques. I would also like to highlight the new results based on small volume step-scaling techniques [4, 5] from ALPHA and a new calculation from ETM using RI/MOM renormalization [6] (a variant of the type of calculation described in more detail in Sec. 3.3). These are labelled ALPHA 21 and ETM 21 in Fig. 1, respectively.

3.1 Current-current correlator method

The lattice current-current correlator method was pioneered in [7–9], and in essence consists of comparing time-moments of Euclidean current-current correlators computed on the lattice with the predictions of high-order perturbation theory. The correlators (and moments) needed are

straightforward to compute on the lattice. The Euclidean-time twopoint function is given by

$$G(t) = a^6(am_{0h})^2 \sum_{\mathbf{x}} \langle J_5(t,\mathbf{x}) J_5(0,0)\rangle \,. \tag{1}$$

where $J_5 \equiv \bar{\psi}_h \gamma_5 \psi_h$ and am_{0h} is the bare quark mass parameter in lattice units. The quantity in brackets is simply the pseudoscalar heavyonium $h\bar{h}$ two-point correlator, from which the particle mass and decay constant would be extracted in a "typical" lattice calculation. Here am_{0h} is an input mass that can be chosen to correspond to the charm mass, but as will be seen it is also convenient to allow this mass to vary from charm to bottom. In formalisms with sufficient chiral symmetry, the current J_5 is absolutely normalized, so that no auxiliary calculation of matching factors is needed. The combination in Eq. (1) is additionally UV finite, so that the lattice computed quantity is equal to its continuum counterpart up to discretization artifacts,

$$G(t)_{\text{cont}} = G(t)_{\text{latt}} + O(a^2) \qquad (t \neq 0) \,. \tag{2}$$

Using this two point calculation the time moments are constructed,

$$G_{n,\text{latt}} = \sum_{t=0}^{T} (t/a)^n \, G(t)_{\text{latt}} \,, \tag{3}$$

which for a given lattice ensemble and input mass am_{h0} give a set of pure numbers indexed by n. These time moments have also been computed in continuum perturbation theory to N^{3}LO [10–12], and they are sensitive to the renormalized quark masses. For $n \geq 4$,

$$G_{n,\text{pert}} = \frac{g_n(\alpha_{\overline{\text{MS}}}, \mu)}{(am_h(\mu))^{n-4}} \,, \tag{4}$$

where $m_h(\mu)$ is the $\overline{\text{MS}}$ quark mass at the scale μ. The goal then is to find the values for $\alpha_{\overline{\text{MS}}}(\mu)$ and $m_h(\mu)$ so that the $G_{n,\text{pert}}$ agree with the lattice data $G_{n,\text{latt}}$, up to discretization artifacts.

In practice HPQCD carries out the analysis in terms of reduced moments which are simply related to the time-moments as

$$R_4 = G_4/G_4^{(0)} \tag{5}$$

$$R_n = \frac{1}{m_{0c}} (G_n/G_n^{(0)})^{1/(n-4)} \quad (n \geq 6) \,. \tag{6}$$

where $G_n^{(0)}$ are the tree-level results for the moments. This has technical advantages including reducing lattice-spacing, tuning, and perturbative errors. In continuum perturbation theory,

$$R_4 = r_4(\alpha_{\overline{\text{MS}}}, \mu) \tag{7}$$

$$R_n = \frac{1}{m_c(\mu)} \, r_n(\alpha_{\overline{\text{MS}}}, \mu) \quad (n \geq 6) \,. \tag{8}$$

Here r_n are the perturbative expressions derived from appropriate powers of $g_n/g_n^{(0)}$, with $g_n^{(0)}$ the lowest order perturbative result. Taking $\mu = 3m_h(\mu)$ in the analysis, for a given m_{0h} one computes the values of R_n from Eq. (6) and gets an estimate of $m_c(3m_h) = R_n/r_n(3m_h)$, via Eq. (8), and in this way both the value and scale dependence of $m_c(\mu)$ can be determined.

Results of this procedure from [7] are reproduced in Fig. 2. One sees that the low moment data has noticeable lattice artifacts, and that by $n = 10$ lattice artifacts are sufficiently small that the data collapses onto gray curve which gives the perturbative evolution.

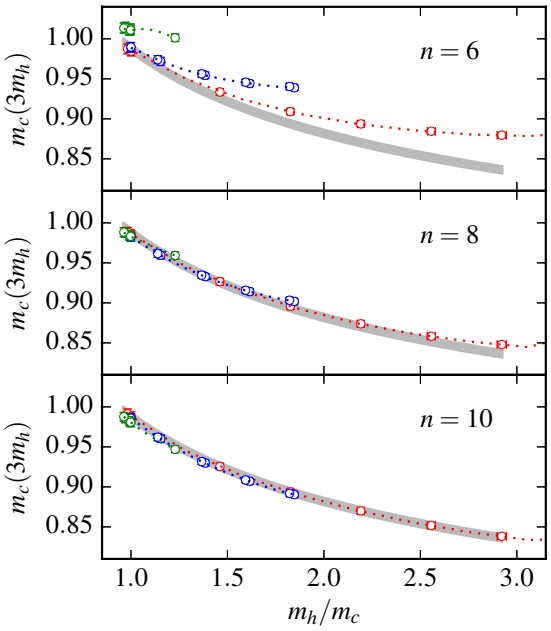

Figure 2: Results of a current-current correlator analysis reproduced from [7]. The colored circles give the lattice data from reduced moments at successively finer lattice spacings, while the gray band shows the best-fit value of m_c evolved using perturbation theory. Discretization artifacts are evident in the data for low moments but by $n = 10$ the data has essentially collapsed onto the perturbative curve.

3.2 MRS masses

This new entrant to the theorist's toolkit [13, 14] takes as its departure point the factorization of heavy meson masses into heavy and light degrees of freedom based on Heavy Quark Effective Theory (HQET):

$$M_H = m_Q + \overline{\Lambda} + \frac{\mu_\pi^2}{2m_Q} - \frac{\mu_G^2(m_Q)}{2m_Q} + \cdots , \tag{9}$$

Here m_Q is the pole mass of the heavy quark Q and $\frac{\mu_\pi^2}{2m_Q}$ its kinetic energy, while the next two terms parameterize light degrees of freedom in the meson, namely the energy of light quarks and gluons $\overline{\Lambda}$ and $\frac{\mu_G^2(m_Q)}{2m_Q}$ the hyperfine energy due to heavy quark spin.

The Fermilab Lattice, MILC and TUMQCD collaborations [15] map out the heavy meson mass dependence on lattice input quark mass from D to B, using a fictitious valence mass $m_{h,0}$, this data forms the main input to their fits. What one desires is however not how the heavy meson mass depends on the bare input mass, but how the heavy meson mass depends on the $\overline{\text{MS}}$ renormalized mass (or equivalently how the $\overline{\text{MS}}$ quark mass depends on the known meson masses). Evaluating this function using the precisely known meson masses m_{D_s}, m_{B_s} will then give the charm, bottom quark mass respectively. This is where Eq. (9) comes in. The challenge then lies in relating the pole mass to the desired $\overline{\text{MS}}$ mass.

The perturbative series connecting the pole mass to the $\overline{\text{MS}}$ mass diverges due to renormalons [13, 14], but in the context of Eq. (9) the authors introduce another mass definition, the

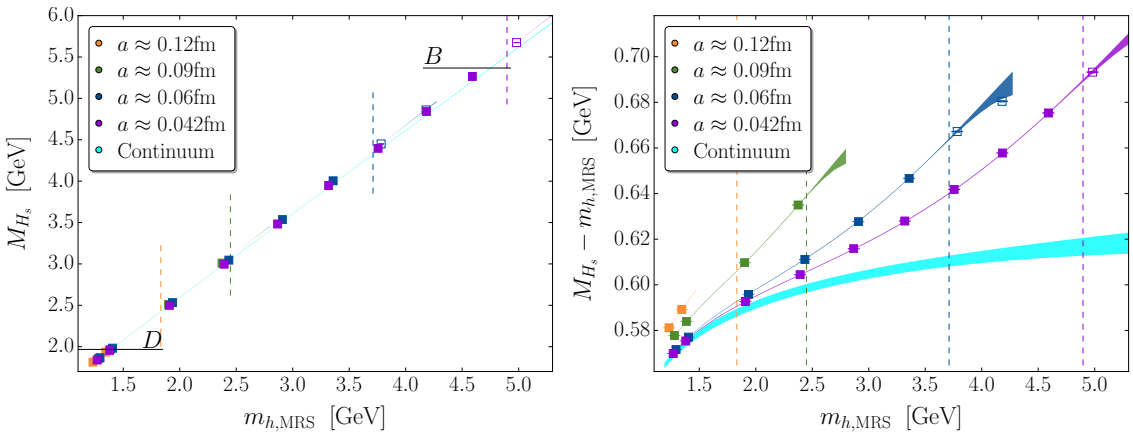

Figure 3: (Left) Fit of lattice determined heavy meson masses to Eq. (9), reproduced from [15]. (Right) Data and fit result with the leading term $m_{h,\mathrm{MRS}}$ subtracted. From this one clearly sees the lattice discretization effects, and the continuum determination of the subleading terms in Eq. (9) from the lattice data given by the blue band.

so-called minimal renormalon subtracted (MRS) mass, which removes the leading renormalon ambiguity from the pole mass and has a well-behaved connection to the $\overline{\mathrm{MS}}$ scheme.

$$\begin{aligned} m_{\mathrm{pole}} + \overline{\Lambda} = \overline{m}\left(1 + \sum_{n=0}^{\infty} r_n\, \alpha_s^{n+1}(\overline{m})\right) + \overline{\Lambda} \rightarrow \\ \overline{m}\left(1 + \sum_{n=0}^{\infty} [r_n - R_n]\, \alpha_s^{n+1}(\overline{m})\right) + J_{\mathrm{MRS}}(\overline{m}) + \left[\delta_m + \overline{\Lambda}\right] \\ = m_{\mathrm{MRS}} + \overline{\Lambda}_{\mathrm{MRS}}\,, \end{aligned}$$

where J_{MRS} sums the $R_n\, \alpha_s^{n+1}$ series, and can be computed from a convergent series in $1/\alpha_s$.

The effectiveness of expressing Eq. (9) in terms of the MRS mass can be seen from the series coefficients r_n and R_n:

$$\begin{aligned} r_n &= (0.4244, 1.0351, 3.6932, 17.4358, \dots) \\ R_n &= (0.5350, 1.0691, 3.5966, 17.4195, \dots) \\ r_n - R_n &= (-0.1106, -0.0340, 0.0966, 0.0162, \dots)\,. \end{aligned}$$

Although individually poorly behaved as n increases, the difference $r_n - R_n$ relating the MRS mass to the pole mass is well under control. In this way the fit form can be expressed in terms of the MRS (or equivalently $\overline{\mathrm{MS}}$) mass.

Fitting the data to Eq. (9) is shown in Fig. 3. Since the "signal" in this figure is just the linear heavy mass dependence, it is instructive to consider a plot of $M_{H_s} - m_{h,\mathrm{MRS}}$. Here the lattice artifacts become clearly visible, and the continuum extrapolation of this data determines the additional continuum terms in Eq. (9).

3.3 RI/(S)MOM

While the previous two methods are tailored specifically to quark masses (and α_s for current-current correlators), the method of non-perturbative renormalization is a very general technique used for renormalizing operators in lattice field theory [16]. Here we consider its application to quark masses using staggered fermions [17].

The main observation is that off-shell momentum subtraction schemes can be directly implemented on the lattice (unlike the $\overline{\text{MS}}$ scheme), provided that the intermediate renormalization scale μ is well below the lattice cutoff (otherwise lattice artifacts will be large), and that a perturbative calculation in the continuum can be used to then convert to $\overline{\text{MS}}$, provided μ is in the "perturbative" regime.

$$\Lambda_{\text{QCD}} \ll \mu \ll \pi/a \tag{10}$$

In practice, the precision application of this technique is aided by theoretical and technical improvements, such as using a "symmetric" subtraction point [18] and twisted boundary conditions [19], as well as access to ensembles at many different lattice spacings, which in this case are made available by the MILC collaboration. In concert these improvements allow one to effectively widen the window condition and separately disentangle both discretization artifacts and non-perturbative contributions.

RI/SMOM schemes were used with staggered fermions in [20] to achieve percent-level precision for m_c. The main result is illustrated in Fig. 4. The computation was carried out using three lattice spacings down to $a \approx 0.06$ fm. The different colored lines in the figure correspond to different choices for the intermediate renormalization scale μ. The increasing slope of these lines is due to $(a\mu)^2$ lattice artifacts, and the curvature at larger μ shows presence of a^4 effects. That these these lines do not converge to a single point at $a = 0$ indicates the presence of non-perturbative effects, which are suppressed at increasing μ values. The final result for $m_c(3\text{ GeV})$ is given by the gray dot on the left and compared with the current-current correlator result.

3.3.1 Perturbative matching

Perturbative matching factors, computed in the continuum, are a key ingredient for these determinations, used to relate the lattice-determined mass renormalization constant to the conventional $\overline{\text{MS}}$ scheme.

$$m_c^{\overline{\text{MS}}} = C_m^{\overline{\text{MS}}/\text{SMOM}}(\mu) Z_m^{\text{SMOM}}(\mu) m_{c,0} \tag{11}$$

In 2018 the SMOM $\to \overline{\text{MS}}$ conversion factor, known at $O(\alpha_s^2)$ [21, 22], was a leading source of uncertainty with the unknown $c_\alpha \alpha_s^3$ term estimated at 0.22% from the fit shown in Fig. 4. This term was subsequently calculated by two sets of authors in [23] and [24],

$$C_m^{\overline{\text{MS}}/\text{SMOM}}(n_f = 4, 3\text{ GeV}) = 1 - 0.01307 - 0.00269 - 0.00196 \tag{12}$$

and an update of the result estimates the new $c_\alpha \alpha_s^4$ at $\approx 0.1\%$.

3.3.2 Adding QED

To really go beyond this level of precision, one must contend with the effects of QED, which could naively be as large as 1%. The effects of (quenched) QED were quantified in the RI/SMOM

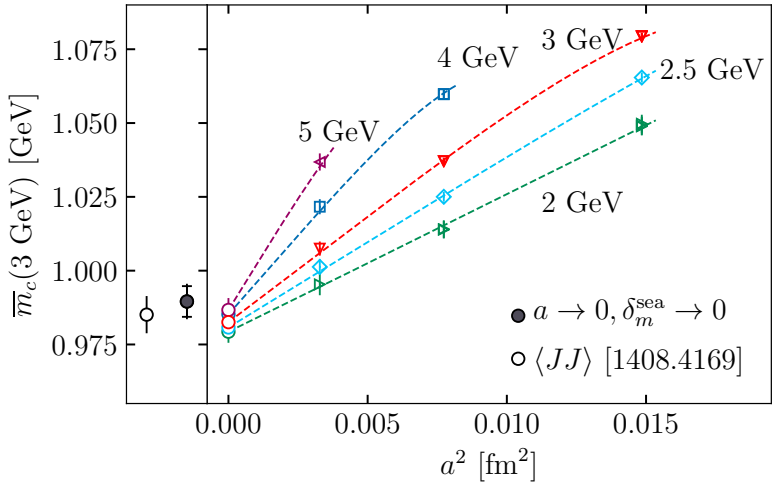

Figure 4: Determination of $m_c^{\overline{\mathrm{MS}}}(3\ \mathrm{GeV})$ based on the RI/SMOM intermediate scheme using highly improved staggered fermions, reproduced from [20]. The calculation was carried out at three lattice spacings and a range of intermediate scales $\mu \in [2, 5]$ GeV to quantify discretization and condensate effects. The final result is given by the gray point on the left and compared with the result based on current-current correlators [7].

framework by extending [20] in [25] and [26] for m_c and m_b respectively. In this approximation the QED field is simply multiplied into the SU(3) gauge field. The effect of the quenching approximation neglects terms of size $\alpha_s^2\alpha$, and so is expected to be maybe 10% of the overall tiny correction. The effect of strong isospin breaking is also neglected, which for the quantities considered is expected to be sub-0.1% [25]. The overall effect of electromagnetism decreases m_c by 0.18(2)%, while the ratio m_b/m_c was found to increase by 0.17(3)%, confirming that the neglect of these corrections is permissible at the percent-level, but becomes significant beyond that.

4. Bottom quark mass

There are 5 new lattice determinations of the bottom mass since 2015 (bringing the total to 9), and one since the 2019 FLAG review. The FLAG review gives an average

$$m_b^{\overline{\mathrm{MS}}}(m_b) = 4.198(12) \qquad (n_f = 2{+}1{+}1)\,, \tag{13}$$

corresponding to a 0.3% uncertainty! The results entering this average are shown in Fig. 5, plus the new result published since the FLAG review from HPQCD [26]. The HPQCD result comes from a determination of the mass ratio m_b/m_c, including the effects of (quenched) QED, multiplied by the determination of m_c via RI/SMOM described in Sec. 3.3. It is in agreement with the FLAG average (as well as with the earlier HPQCD result without QED effects), showing that QED effects are tiny for this quantity.

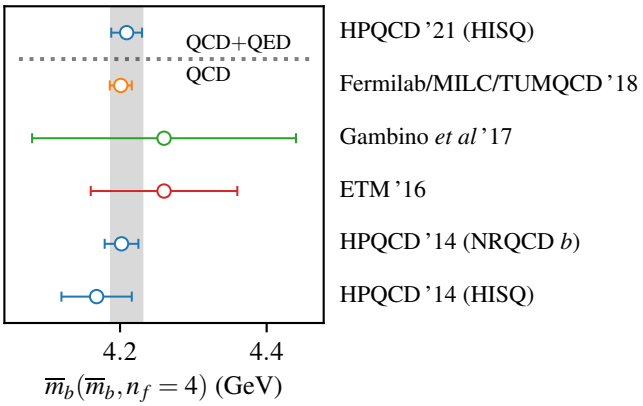

Figure 5: Summary plot of $n_f = 4$ $m_b^{\overline{\rm MS}}(m_b)$ results from lattice QCD, reproduced from [26]. The result HPQCD 21, published since the 2019 FLAG review, includes the effects of (quenched) QED.

5. Summary & Conclusion

Since Charm 2015 there has been significant progress made in the computation of heavy quark masses from lattice. For one thing, there are many new results – I count 13 since 2015, and 4 since the most recent FLAG review. These come from several different collaborations using different lattice discretizations, which gives confidence that lattice artifacts are under control. But perhaps more importantly, there are now a variety of different techniques being used, and the agreement among methods gives confidence that sources of systematic uncertainty particular to each method are being well-estimated. This establishes the masses at the (sub-)percent level. At this level of precision one may expect QED effects to become relevant. These were quantified in [25] and [26], and found to be small ($\lesssim 0.2\%$ for charm).

I've focused here on a few of the recent calculations quoting small uncertainties, emphasizing the differing methodologies used. However, the good agreement between results is not without caveats. The main one being the three calculations highlighted here are based on simulations with HISQ fermions, and use the same sets of FNAL-MILC ensembles. It will be interesting in the future to see how results using different regularizations compare. The methods highlighted here are also not the only ones on the market. In particular small volume step-scaling techniques provide a promising avenue to precision quark masses and are continuing to evolve. Surely there are additional variants, as well as brand new ideas, waiting to be discovered.

6. Acknowledgements

I would like to express my gratitude to the organizers for an enjoyable conference and their hard work ensuring that the conference could go forward. I would also like to thank Andreas Kronfeld for providing helpful comments on the manuscript.

References

[1] G. P. Lepage, P. B. Mackenzie and M. E. Peskin, arXiv:1404.0319 [hep-ph].

[2] S. Aoki *et al.* [Flavour Lattice Averaging Group], Eur. Phys. J. C **80**, no.2, 113 (2020) doi:10.1140/epjc/s10052-019-7354-7 [arXiv:1902.08191 [hep-lat]].

[3] A. T. Lytle, Contribution to CHARM 2015, [arXiv:1509.03078 [hep-lat]].

[4] J. Heitger *et al.* [ALPHA], JHEP **05**, 288 (2021) doi:10.1007/JHEP05(2021)288 [arXiv:2101.02694 [hep-lat]].

[5] I. Campos *et al.* [ALPHA], Eur. Phys. J. C **78**, no.5, 387 (2018) doi:10.1140/epjc/s10052-018-5870-5 [arXiv:1802.05243 [hep-lat]].

[6] C. Alexandrou, S. Bacchio, G. Bergner, M. Constantinou, M. D. Carlo, P. Dimopoulos, J. Finkenrath, E. Fiorenza, R. Frezzotti and M. Garofalo, *et al.* [arXiv:2104.13408 [hep-lat]].

[7] B. Chakraborty *et al.*, Phys. Rev. D **91** (2015) 5, 054508 [arXiv:1408.4169 [hep-lat]].

[8] I. Allison *et al.* [HPQCD], Phys. Rev. D **78**, 054513 (2008) doi:10.1103/PhysRevD.78.054513 [arXiv:0805.2999 [hep-lat]].

[9] C. McNeile, C. T. H. Davies, E. Follana, K. Hornbostel and G. P. Lepage, Phys. Rev. D **82** (2010) 034512 [arXiv:1004.4285 [hep-lat]].

[10] K. G. Chetyrkin, J. H. Kuhn and C. Sturm, Eur. Phys. J. C **48** (2006) 107 [hep-ph/0604234].

[11] R. Boughezal, M. Czakon and T. Schutzmeier, Phys. Rev. D **74** (2006) 074006 [hep-ph/0605023].

[12] A. Maier, P. Maierhofer, P. Marquard and A. V. Smirnov, Nucl. Phys. B **824** (2010) 1 [arXiv:0907.2117 [hep-ph]].

[13] J. Komijani, JHEP **08**, 062 (2017) doi:10.1007/JHEP08(2017)062 [arXiv:1701.00347 [hep-ph]].

[14] N. Brambilla *et al.* [TUMQCD], Phys. Rev. D **97**, no.3, 034503 (2018) doi:10.1103/PhysRevD.97.034503 [arXiv:1712.04983 [hep-ph]].

[15] A. Bazavov *et al.* [Fermilab Lattice, MILC and TUMQCD], Phys. Rev. D **98**, no.5, 054517 (2018) doi:10.1103/PhysRevD.98.054517 [arXiv:1802.04248 [hep-lat]].

[16] G. Martinelli, C. Pittori, C. T. Sachrajda, M. Testa and A. Vladikas, Nucl. Phys. B **445**, 81-108 (1995) doi:10.1016/0550-3213(95)00126-D [arXiv:hep-lat/9411010 [hep-lat]].

[17] A. T. Lytle and S. R. Sharpe, Phys. Rev. D **88**, no.5, 054506 (2013) doi:10.1103/PhysRevD.88.054506 [arXiv:1306.3881 [hep-lat]].

[18] C. Sturm, Y. Aoki, N. H. Christ, T. Izubuchi, C. T. C. Sachrajda and A. Soni, Phys. Rev. D **80**, 014501 (2009) doi:10.1103/PhysRevD.80.014501 [arXiv:0901.2599 [hep-ph]].

[19] R. Arthur *et al.* [RBC and UKQCD], Phys. Rev. D **83**, 114511 (2011) doi:10.1103/PhysRevD.83.114511 [arXiv:1006.0422 [hep-lat]].

[20] A. T. Lytle *et al.* [HPQCD], Phys. Rev. D **98**, no.1, 014513 (2018) doi:10.1103/PhysRevD.98.014513 [arXiv:1805.06225 [hep-lat]].

[21] M. Gorbahn and S. Jager, Phys. Rev. D **82**, 114001 (2010) doi:10.1103/PhysRevD.82.114001 [arXiv:1004.3997 [hep-ph]].

[22] L. G. Almeida and C. Sturm, Phys. Rev. D **82**, 054017 (2010) doi:10.1103/PhysRevD.82.054017 [arXiv:1004.4613 [hep-ph]].

[23] B. A. Kniehl and O. L. Veretin, Phys. Lett. B **804**, 135398 (2020) doi:10.1016/j.physletb.2020.135398 [arXiv:2002.10894 [hep-ph]].

[24] A. Bednyakov and A. Pikelner, Phys. Rev. D **101**, no.9, 091501 (2020) doi:10.1103/PhysRevD.101.091501 [arXiv:2002.12758 [hep-ph]].

[25] D. Hatton *et al.* [HPQCD], Phys. Rev. D **102**, no.5, 054511 (2020) doi:10.1103/PhysRevD.102.054511 [arXiv:2005.01845 [hep-lat]].

[26] D. Hatton, C. T. H. Davies, J. Koponen, G. P. Lepage and A. T. Lytle, Phys. Rev. D **103**, no.11, 114508 (2021) doi:10.1103/PhysRevD.103.114508 [arXiv:2102.09609 [hep-lat]].

[27] N. Carrasco *et al.* [European Twisted Mass Collaboration], Nucl. Phys. B **887** (2014) 19 [arXiv:1403.4504 [hep-lat]].

[28] Y. B. Yang *et al.*, Phys. Rev. D **92** (2015) 3, 034517 [arXiv:1410.3343 [hep-lat]].

[29] Z. Liu *et al.* [chiQCD Collaboration], Phys. Rev. D **90** (2014) 3, 034505 [arXiv:1312.7628 [hep-lat]].

[30] B. Colquhoun, R. J. Dowdall, C. T. H. Davies, K. Hornbostel and G. P. Lepage, Phys. Rev. D **91** (2015) 7, 074514 [arXiv:1408.5768 [hep-lat]].

[31] A. J. Lee *et al.* [HPQCD Collaboration], Phys. Rev. D **87** (2013) 7, 074018 [arXiv:1302.3739 [hep-lat]].

[32] B. Blossier *et al.* [ETM Collaboration], JHEP **1004** (2010) 049 [arXiv:0909.3187 [hep-lat]].